A METHODOLOGICAL APPROACH TO THE STUDY OF LOCALISED CORROSION

Bruno BAZZONI (*), Bruno MAZZA (*), Dany SINIGAGLIA (*), and Bruno VICENTINI (**).

(*) Centro di Studio CNR sui Processi Elettrodici, Politecnico di Milano, I-02100 Milano

(**)Laboratorio LTM del CNR, Cinisello Balsamo (Milano).

Summary - Some recent studies on localised corrosion using models of occluded cells are surveyed. The chemical and physical principles underlying the "occluded cell" framework allows rationalisation of the methods and techniques of experimental investigation and permits the resistance to localised corrosion of new metallic materials with an active-passive behaviour to be ranked.

Riassunto - Viene presentata una rassegna di recenti studi sulla corrosione localizzata che utilizzano modelli di "cella occlusa". E' opinione degli autori che la discussione sui principi chimici e fisici secondo cui funzionano le celle occluse, possa contribuire in particolare a una razionalizzazione dei metodi e delle tecniche di indagine sperimentale e ad una classificazione più affidabile di nuovi materiali metallici a comportamento attivo-passivo in base alla loro resistenza alla corrosione localizzata.

INTRODUCTION

The present knowledge of the different forms of localised corrosion emphasises some phenomenological aspects common to them, such as the formation of concentrated solutions in sites where alloy dissolution proceeds, the progressive acidification of the anodic

region caused by metal-cation hydrolysis, the presence of an uneven electric potential distribution, and the effect of intrinsic defects in the material such as non-metallic inclusions. Hence, the interest in studying morphologically different forms of corrosion - i.e. pitting, crevice corrosion, stress corrosion, filiform corrosion - according to an overall view[1]. This has developed, via the idea of an occluded cell, seen as a limited portion of solution adjacent to the surface of the corroding alloy, which only with difficulty can exchange matter with the bulk of the solution. Figure 1 shows a series of aspects and phenomena linked with the electrochemical working of an occluded cell. It is necessary to take into account the above-mentioned aspects and phenomena to describe in a more precise way the initiation and development of localised corrosion.

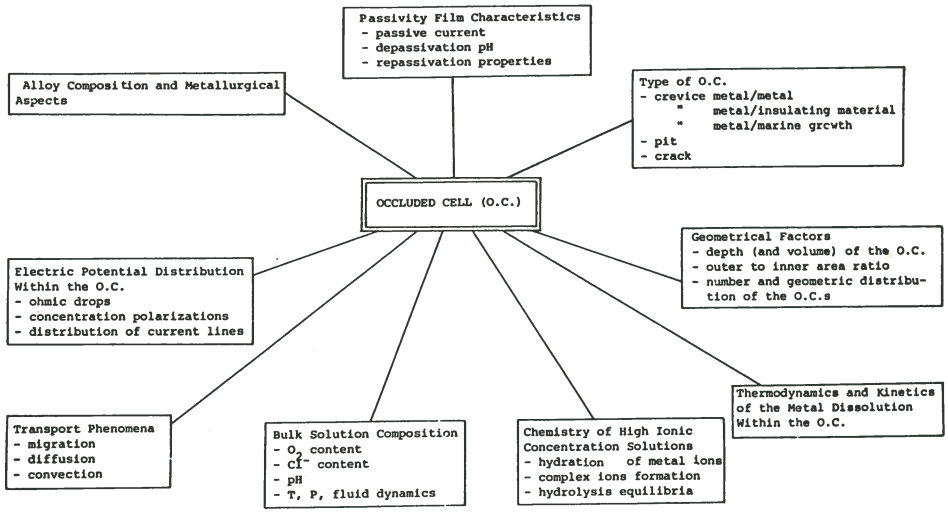

FIG. 1 - Factors and phenomena affecting localised corrosion.

In this paper we survey some recent studies on localised corrosion using occluded cell models. Some of these models are means for estimating quantities characterising the localised corrosion phenomenon and involve difficult experimental determination. Others

are more elaborate mathematical models, which reproduce a particular mechanism of localised corrosion. If backed up by adequate experimental checks, the latter are useful for predicting the localised corrosion resistance of a metallic structural element in given conditions at the design stage (choice of materials).

We notice that the debate about the chemical and physical principles according to which the occluded cells work, contributes to rationalising methods and techniques of experimental research. In particular, the work reviewed here shows how useful it is to have available a methodology which develops both the experimental and theoretical investigation of the phenomena, and the study and estimate of considered quantities by mathematical models.

MATHEMATICAL MODELS AND EXPERIMENTAL STUDIES

Faita et al.[2] examined different aspects of localised corrosion referring to an occluded cell operating in the presence of high ionic concentrations. The formation of concentrated solutions is explained on the grounds of the electrochemical working of the occluded cell. During the initial stages of cell activity, the transport of ionic species is exclusively by migration, which predominates over diffusion because concentration gradients have not yet been established (transport by convenction is not considered throughout this paper). The assumptions underlying the calculations are:

i) the occluded cell is cylindrical in shape (figure 2a) with only the bottom surface an anodic area;
ii) the bulk solution contains the binary electrolyte AX at initial concentration C_o;
iii) the corrosion process makes monovalent metal ions M^+ go into solution;
iv) migration makes the cations move away from the occluded cell and the anions inside it;
v) ionic mobilities have the same value irrespective of the nature and concentration of ions.

The calculations consist in obtaining concentrations C_{M^+}, C_{A^+}, C_{X^-} of ionic species M^+, A^+, and X^-, respectively, in the occluded cell (^) as a function of the circulating electric charge, q. The concentration of salt MX in the occluded cell grows (see figure 2b).

(^) Concentrations are assumed to be uniform in the occluded cell.

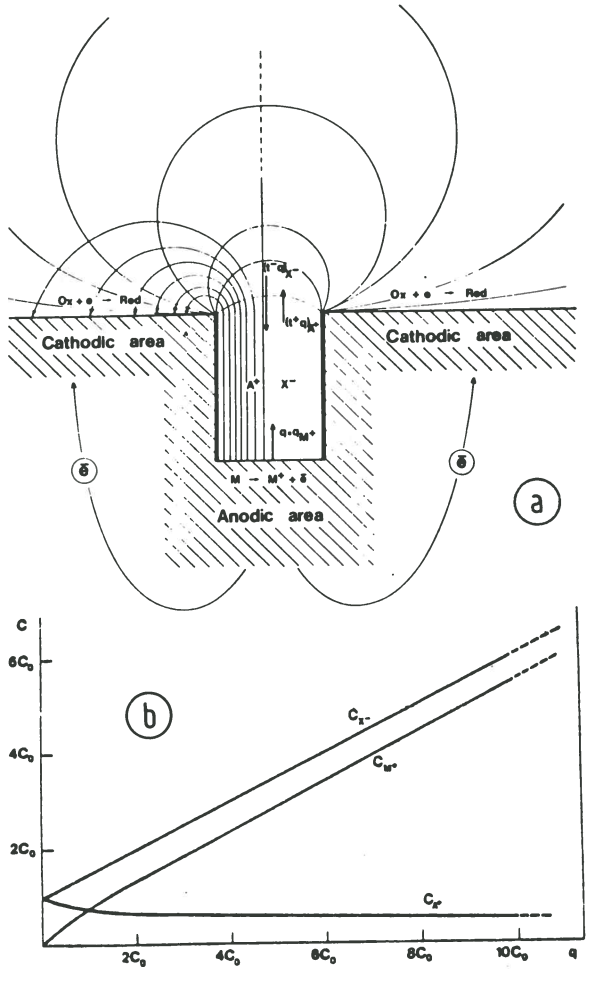

FIG. 2 - a) Phenomena inside an occluded cell, simplified model.

b) Concentration changes whithin an occluded cell as a function of the electric charge, q. q is measured in C_o units, C_o being the concentration of the electrolyte AX in the starting solution[2].

Ions of the corroding metal or alloy (Fe^{2+}, Cr^{3+}, Ni^{2+}, Al^{3+} etc.) generally have small ionic radius and high electric charge, and so are able to coordinate a large number of water molecules. High hydration endows them with a lower mobility than for the anions; hence the tendency of the alloy cations to accumulate near the anodic area. Hydration and hydrolysis reactions "consume" water and consequently decrease the ratio H_2O/ionic species (11 water molecules for saturated $FeCl_2$, 16 for saturated $AlCl_3$, etc.). According to the authors[2], this affects both the thermodynamics and kinetics of the metal dissolution reaction: e.g. as in non-aqueous solvents, it may oppose the formation or the healing of passive films (of which water is an important constituent). In conclusion, the authors[2] acknowledge that the key to a deeper knowledge of the phenomena taken into account, are the studies of physical chemistry of concentrated solutions and of the metal anodic behaviour as a function of water content and halide concentration.

Pickering and Frankenthal[3,4] applied the equation of diffusion and migration transport in dilute solutions[5-7] to an occluded cell (pit type) to calculate the concentration profiles of different ionic species in steady-state conditions. An occluded cell of cylindrical shape (like the previous one) was assumed with inert passive walls. Metal dissolution, $M_{(s)} \rightarrow M^+_{(aq)} + e^-$, takes place on the bottom whilst the mass flows take place parallel to the length of the cell. The solution is assumed to consist of a binary acid-electrolyte mono-monovalent H^+Y^-, where Y^- is a non-complexing, aggressive anion The calculation consists in the analytic solution of transport equations written for the chemical species H^+, Y^- and M^+, together with the electroneutrality equation and the boundary conditions; the expressions of the potential distribution $\emptyset$ and of the concentrations of H^+, Y^- and M^+ (C_{H+}, C_{Y-} and C_{M+}) along the depth x of the occluded cell, were obtained. Figure 3a shows the curves of the given quantities as a function of the product $i_M x$ (A cm^{-1}), where i_M is the current density of metal dissolution and x is the occluded cell depth measured from its mouth. The diffusion coefficient was assigned a single value, 10^{-5} cm^2 s^{-1}, and the bulk concentration C° of electrolyte H^+Y^- a value of 1 mol l^{-1}. C_{M+} goes up as i_M or x grow, given that the dissolution reaction takes place only at the bottom of the pit. C_{Y-} grows, whereas C_{H+} falls depending on the tendency of anions to move towards the bottom of the occluded cell, and of cations to move the opposite way. The resultant effect is the formation of a highly concentrated solution of salt M^+Y^-, which eventually precipitates; the dotted lines in figure 3a refer to the case of salt precipitation in the occluded cell.

The authors[3] proposed some experimental methodologies for measuring the potential distribution inside a pit using a Luggin-Haber microprobe. Figure 3b shows the calculated and measured potential curves in an iron pit, along the depth; the agreement between the two curves is good except for the portion near the

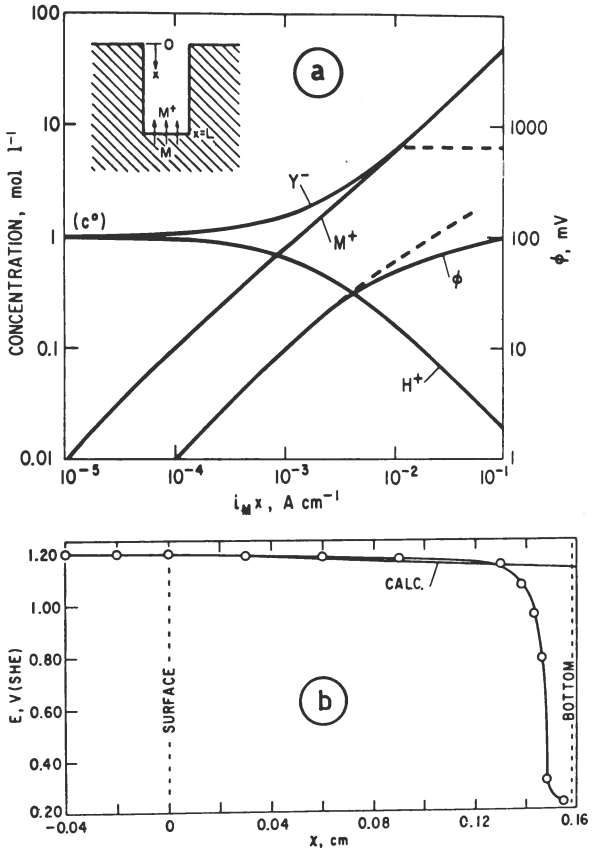

FIG. 3 - a) Calculated concentrations of Y^-, H^+ and M^+ and potential Ø as a function of the product of the depth x and the current density $i_M \cdot C^\circ$ is the bulk concentration of acid HY.
b) Plot of measured potentials as a function of depth x into the pit for a single-pit iron specimen in 0.5 mM H_2SO_4 + 0.5 M Na_2SO_4 + 2 mM NaCl (pH 3.9) solution. Calculated potentials $/\bar{E}(x) = E(x=0) - Ø(x)/$ are given for comparison. For x > 0.13 cm, measured potentials are the least noble ones[3].

occluded cell bottom, where the potential measured decreases sharply, not foreseen in the calculations. According to the authors[3], this may be ascribed to the development of small bubbles which block

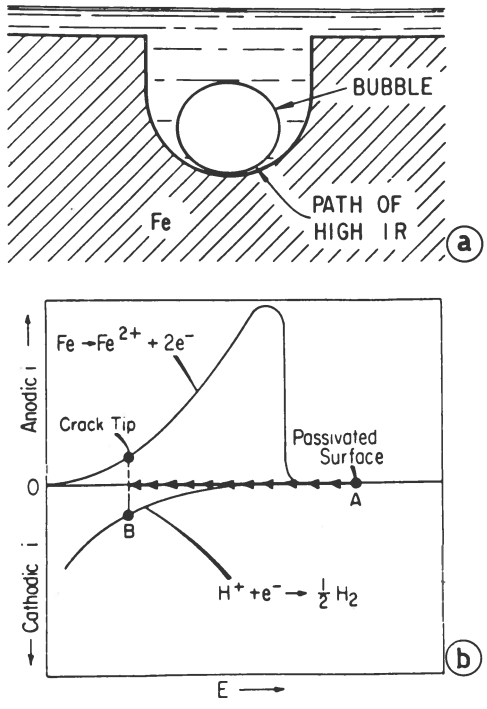

FIG. 4 - a) Schematic of a pit illustrating a high-resistance electrolyte path caused by a bubble[3].
b) Schematic which shows that during pitting the electrode potential shifts from A at the passivated outer surface to less noble values in the pit, and that both hydrogen evolution and metal dissolution could occur within the pit[8].

up the occluded cell (figure 4a) and cause a sharp ohmic drop. The small bubbles liberated from quite a lot of pits were collected and analysed; the gas was found to be hydrogen. As illustrated in figure 4b[8], this generates on the bottom of the pit even when the potential imposed on the outside is considerably more anodic than that thermodynamically required for the reduction of H^+ ions in acid solutions.

Galvele[9] studied the transport processes in an occluded cell of cylindrical shape having passive walls like the previous ones, introducing some modifications to the Pickering model. These modifications consist in taking into account the hydrolysis reac-

tion (^), in introducing the initial pH (bulk value) among the boundary conditions, and in considering that the inert electrolyte, NaCl in the case dealt with, present in the solution, acts as a supporting electrolyte for the metallic ions and the hydrolysis products which form. This last hypothesis allows the authors to look at the problem considering exclusively the diffusion transport. The system is described following a procedure already illustrated by Vetter[10] and leads, in steady conditions, to the analytic expressions of the species M^{z+}, $M(OH)^{(z-1)+}$, H^+ still as a function of the product $i_M x$ (A cm^{-1}). In Figure 5 it is given as an example the graph relative to the localised corrosion of chromium. The upper line shows the total concentration of all species containing chromium atoms and it becomes horizontal for $C_{Cr^{3+}}$ = 10 mol l^{-1} as a consequence of the metal salt precipitation. In addition, if $C^{\circ}_{H^+} = 10^{-7}$ mol l^{-1} as in the graph shown, C_{H^+} grows, that is to say that the pH falls as the product $i_M x$ goes up: the lowest pH values will be reached in the deepest portion of the occluded cell.

The diagrams are discussed according to the criterion of concentration H^+ critical, following approximately what already adopted in Pourbaix diagrams. That is: if the oxide solubility product determining the metal passivity is known, from the equilibrium data of the reaction $M^{z+} + z/2\ H_2O \rightleftharpoons MO_{z/2} + z\ H^+$ the critical value of the pH (shown on the graph of figure 5 by a cross) at which the oxide is in equilibrium with a solution containing traces of metal (10^{-6} mol l^{-1}) can be calculated. At lower pH, the oxide is soluble, and is therefore not protective. For a more accurate use of the graphs, one can refer to the experimental determination of critical pH for depassivation of the metal (see below). Diagrams such as that for chromium show that for many metals the critical pH is obtained for values of $i_M x$ lower than 10^{-6} A cm^{-1}. Consequently, since in the conditions of pits initiation current density values of 1 A cm^{-2} are reached, it is possible to conclude that one can obtain the acidification necessary for the development of occluded cells in pits 10^{-6} cm deep. A crack in a thin film (such as a passive film) is sufficient to give a diffusion path long enough to reach the critical pH. If there are cracks in the passive film, but the current density is not sufficiently high, it is necessary only to apply potentials, even shortly, noble enough to reach current density values above mentioned.

Vicentini *et al.*[11] calculated the potential distribution inside a crevice of defined geometry, in which active and passive states of the metallic materials may co-exist; this is the case of stainless steels, titanium, etc. The model precisely describes situations of propagation rather than initiation of corrosion in a

---

(^) According to the equation $M^{z+} + H_2O \rightleftharpoons M(OH)^{(z-1)+} + H^+$ (equilibrium characterised by the hydrolysis constant).

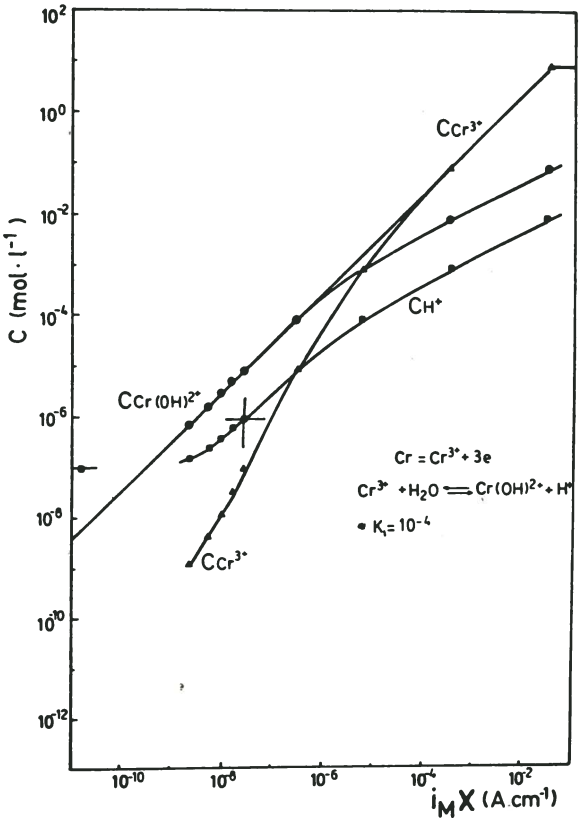

FIG. 5 - Calculated concentrations of Cr^{3+}, $Cr(OH)^{2+}$, and H^{+} as a function of the product of the depth $\underline{x}$ and the current density $\underline{i}_M$ in a unidirectional pit. $\underline{C}^{\circ}_{H^{+}} = 10^{-7}$ mol l^{-1} [9].

crevice. The occluded cell shown in figure 6a, is assumed to be set up between a cylindrical metal sample and a hole obtained from an insulating material. The crevice thickness was considered negligible compared to the length and only the potential distribution along the coordinate $\underline{x}$ of the length was taken into account. On the unshielded metallic surface ($\underline{x}$ = 0) the potential was assumed to be kept at a constant value by a potentiostat, or by a redox system. The solution which fills the gap has a given conductivity and modifications of the chemical composition of the solution were neglected; this means that the concentration gradients set up along the crevice are neglected. The calculation consists in applying Ohm's

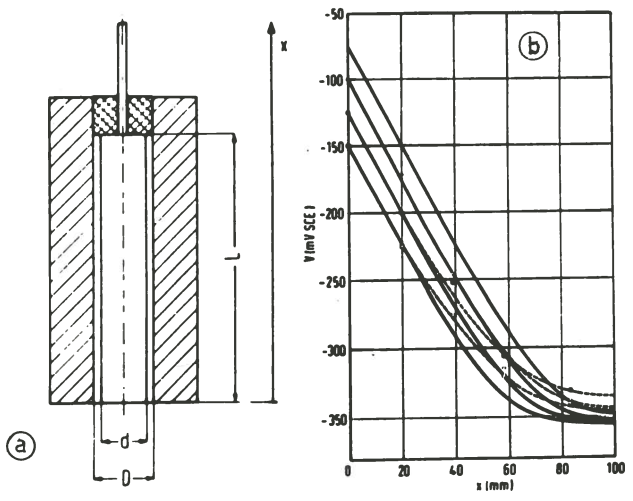

FIG. 6 - a) Schematic assembly of the system used in the study of the crevice corrosion of metallic materials susceptible to active-passive transition[11]. b) Comparison between the experimental (dashed lines) and calculated (full lines) profiles of the potential along the crevice for the AISI 304 and for different values of the potential imposed on the free surface, V_e (□ : V_e = -150 mV; ● : V_e = = -125 mB; o: V_e = -100 mV vs. SCE). Bulk solution: de-aerated 2 M H_2SO_4 at 40 °C [12].

law and the charge balance equation, applying suitable boundary conditions, and analytically and numerically solving the mentioned equations. An approximate analytical (or experimental) expression for the anodic characteristic of the material examined was also introduced.

The authors[12] carried out an experimental check of the results from the calculation using stainless steel and titanium, both susceptible to an active-passive transition. Electrochemical tests made use of a crevice having the same shape as that described in the model; they consisted in measuring the potential in the crevice at different depths (using a probe system) and in observing the trends in dissolution on the sample. Agreement with the calculus results was found (at least in the first period of working of the system) as shown in figure 6b, which refers to the behaviour of

AISI 304 in acid solutions (the calculated curves are compared with those measured along the depth).
One can draw some conclusions which are significant from an engineering point of view, such as the co-existence (made steady by ohmic drops) of active and passive areas along the occluded cell, the knowledge of the passive area length, and hence the necessary conditions to achieve the anodic protection of crevices having simple and known geometry.

Newman et al.[13] approached the calculation of the potential distribution in a hemispherical pit by numerically working out the Laplace equation (which is strictly valid only in solutions without any concentration gradient). The model consisted of a hemispherical pit which corrodes with uniform current density, surrounded by a passive plane surface. Hence, the Laplace equation can be written in spherical coordinates, together with appropriate boundary conditions. Figure 7a shows the results: equipotential surfaces, numerically characterised by a non-dimensional potential $\phi^* = \phi k / i_w r_w$ (where ϕ is the electric potential, k the solution conductivity, i_w the current density at the pit wall, and r_w the pit radius), are reported. Figure 7b shows the normalised potential, ϕ^*, trend from the bottom of the pit along different trajectories; of particular interest is the presence of a high potential gradient on the edge, between the active surface and the passive one.

Crolet and Defranoux[14], evaluated the incubation time of crevice corrosion phenomena of stainless steels. The calculation assumes a mechanism according to which in the occluded cell the solution progressively acidifies (because of hydrolysis of the metallic ions which accumulate) without causing corrosion of the passive material, until a depassivation pH is reached, at which the alloy becomes active and therefore is in a situation of generalised corrosion in acid medium. According to this now widely accepted mechanism, the incubation time becomes an important parameter for defining and preveding crevice corrosion phenomena. Without going into details, the calculation consists of a material balance between the ions entering into the crevice because of alloy dissolution, those leaving the crevice because of electric migration, and those which accumulate in the occluded cell. This balance includes an expression for the hydrolysis equilibrium constant of the Cr^{3+} cations, which alone cause pH decreases in the crevice. A relation between incubation time and pH is obtained; this is a function of the crevice gap, the passive current density, the alloy chemical composition, and the initial pH in the solution. In figure 8 is shown the evolution of pH with time, the latter on linear and logarithmic coordinates. An initial, sharp, pH decrease occurs in the occluded cell which then slows down; this is due to the increasing difficulty of Cr^{3+} hydrolysis. This trend corresponds to experimental observations. The model assumes the experimental measurement of the depassivation pH, which is specific for each alloy with an active-passive transition. The same authors[15] proposed an

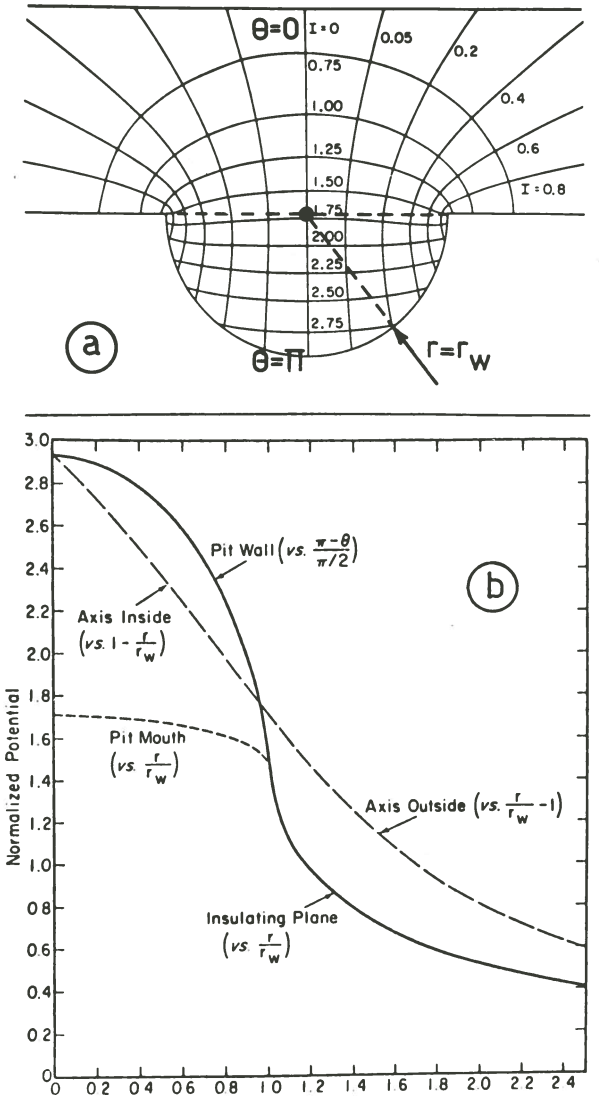

FIG. 7 - a) Normalised equipotentials and flux curves for a corroding pit with uniform current density in the pit and zero current density on the surrounding planar surface. Flux lines show enclosed current divided by total current.
b) Normalised potential gradient on pit surface, on the plane, and along the pit axis[13].

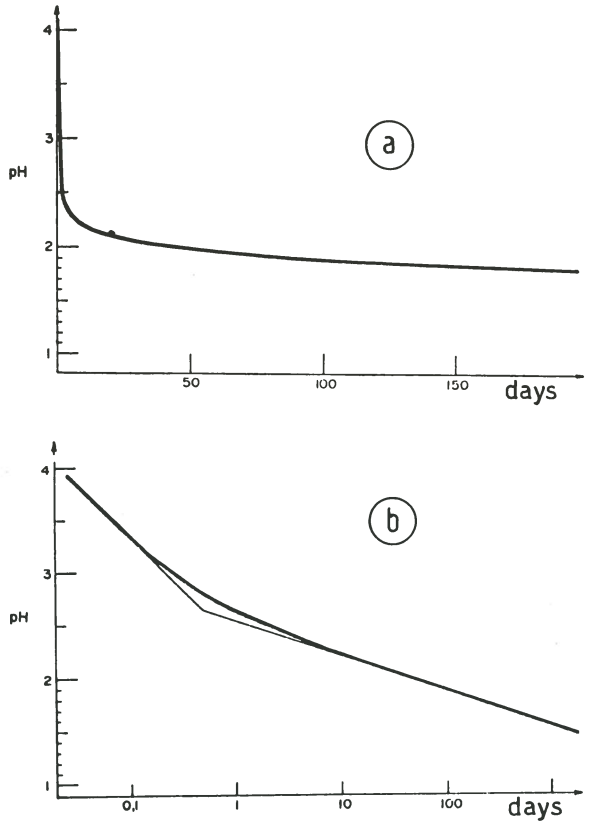

FIG. 8 - Time evolution of pH in crevice. Crevice gap 0.05 mm, chromium content of stainless steel 20%, passive current density 0.1 μA cm^{-2}, starting solution at pH 7[14].

electrochemical method for determining the depassivation pH, which is also useful for classifying different alloys with regard to their susceptibility to crevice corrosion.

Oldfield and Sutton[16] presented a mathematical model of the crevice corrosion of stainless steels in neutral chloride solutions. The procedure consists in formulating a mechanism of the corrosive attack, and representing it by a model of calculation by which some quantities and relations useful in the prediction of trends may be estimated. The mechanism considers four stages, here summarised as follows.

The alloy is assumed to be initially in a passive state, and the solution composition in the crevice the same as that in the bulk (where the unshielded metal is dipped).

1st stage: O_2 depletion, if possible, inside the crevice by cathodic reaction matched locally by an equal anodic passive current.

2nd stage: large-scale separation, due to differential aeration, between cathodic and anodic area; the latter is formed by the alloy surface within the crevice. The passive current produces metal ions (Fe^{2+}, Cr^{3+}, $Ni^{2+}Mo^{3+}$, etc.) which accumulate in the crevice where they hydrolyse and acidify the solution. At this stage, the anion concentration progressively increases to maintain electroneutrality, which increases the aggressiveness of the solution even more.

3rd stage: there is a permanent and general breakdown of the passive film on the alloy surface within the crevice and the onset of rapid corrosion. This happens when the critical crevice conditions in the second stage, expressed in terms of critical pH and of critical concentration of aggressive anion (Critical Crevice Solution, CCS), are reached. Critical conditions are specific for each material-environment system, so they must be determined experimentally for each case.

4th stage: corrosion propagation in the occluded cell, that is rapid dissolution of the "active" alloy balanced by oxygen reduction on the external passive surface and by H^+ reduction inside the crevice, with hydrogen evolution.

The mathematical model describes the first three stages of the corrosion process: the propagation stage and the corrosion rate are not dealt with. Figure 9 lists the input and output data of the model of calculation at each stage. The most detailed stage is the second one which involves calculation (for a crevice obtained between parallel metal-metal or metal-insulator planes) of the time evolution of the pH and of the concentrations of the different chemical species in crevice solution. Utilising computer iteration, the model follows the hydrolysis equilibria as the metal-ion concentrations grow, introducing subsequent corrections which take transport phenomena (migration and diffusion) into account and the effect of H^+ activity increase in concentrated solutions. For this purpose, experimental data of pH measurements in concentrated $FeCl_2$ and $CrCl_3$ solutions, were used[17]. Some of the results are shown in figure 10a and 10b, which refer to an 18 Cr-10Ni-2.5 Mo - type stainless steel: the first gives the pH decrease with time for a value of the passive current density/crevice gap ratio of 10^{-2} A cm^{-3}, and for different crevice depths; the second shows the predicted changes in the composition of the crevice solution as the pH falls.

The same authors[18] experimentally verified the predictions obtained via the model, and determined a series of parameters necessary for utilising the equations (such as the passive current density

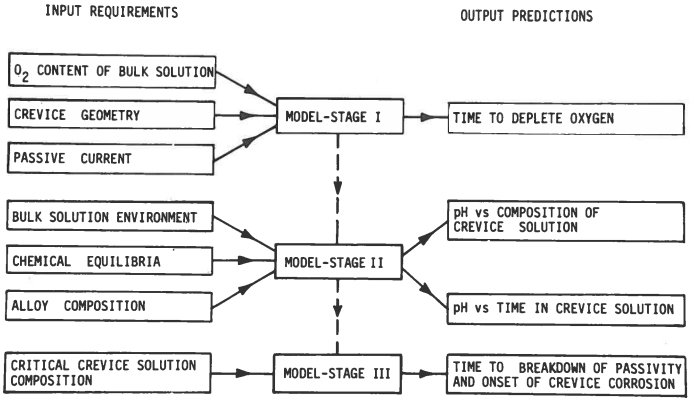

FIG. 9 - General flow chart of mathematical model highlighting the inputs and outputs[16].

and the CCS composition). Figure 11 shows a comparison between "time to breakdown" of passive films, i.e. the incubation time of crevice corrosion, as predicted by the model and observed experimentally; agreement between the two is good.

The mathematical model was used[19] to rank the resistance to crevice corrosion initiation of new alloys in ambient-temperature sea water.

DISCUSSION AND CONCLUSION

Although much of the work reviewed is fragmentary in nature, it brings to light some fundamental aspects for understanding and predicting the behaviour of stainless alloys in aggressive media such as sea water. An overview of localised corrosion phenomena is made difficult by the critical interdipendence of many of the parameters involved.

The importance of transport phenomena in solution is brought out in many discussions on the working mechanism of occluded cells. Analytical treatment of these phenomena leads to results expressed in terms of predicted H^+ -ion, anion and metal-ion concentrations inside occlude cells, which are in substantial agreement with experimental observations[17,20-24]. Further advances require

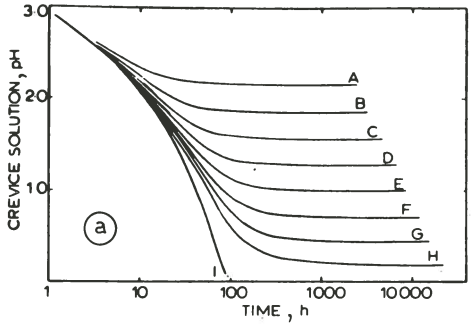

Curve	Crevice depth	Curve	Crevice depth
A	0.3 cm	F	0.8 cm
B	0.4 cm	G	0.9 cm
C	0.5 cm	H	1.0 cm
D	0.6 cm	I	∞
E	0.7 cm		

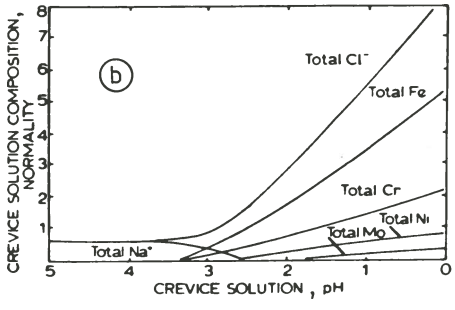

FIG. 10 - a) Predicted combined effect of diffusion and migration on the pH fall in an 18 Cr-10Ni-2.5Mo type stainless steel assuming a value of the passive film current density/ crevice gap ratio of 10^{-2} A cm^{-3} and that the passive film does not breakdown; the curves correspond to a series of crevice depths.
b) Predicted change in crevice solution composition as the pH falls for the same stainless steel in ambient temperature sea water[16].

Crevice geometry		Bulk solution	Time to breakdown, h	
Gap	Area ratio		Predicted	Observed
10 μm	1 : 1	Aerated 1 M NaCl	54	25 - 90
10 μm	20 : 1	Aerated 1 M Nacl	18	5 - 20

FIG. 11 - Comparison of predicted and observed times to breakdown for type AISI 316 crevices[18].

treatment valid for concentrated solutions and, particularly, the introduction of experimentally determined form factors (roughness, minimal interstitial thickness, etc.) in the case of crevice corrosion in order to take into account complex, real geometries.

Another aspect of importance is that concerning the more strictly chemical properties of the solution produced inside the occluded cells and their relation to initiation and propagation of attack. Progressive acidification of the solution is a central idea in all the crevice and pitting corrosion mechanism put forward to date. The formation of an acidic solution is the result of hydrolysis reactions and the formation of hydroxychloro complexes by metal cations. In addition, the existence of strong interactions (mainly electrostatic in nature) between chemical species in the concentrated solutions must be considered. The resultant effect is clearly brought out by the considerable increase (10-100 times, i.e. a decrease of 1-2 pH units) in the activity coefficient of the H^+ ion when chlorides are added to 0.1 m HCl solution (see figure 12)[24].

A more strictly electrochemical aspect is that of the distribution of the electrical potential inside and surrounding the occluded cell (whether interstitial or pitted). The electrical conductance of the solution contributes in determining the ratio between anodic and cathodic areas and hence the penetration rate of the attack. However, difficulties arise due to the possibility that passive (cathodic) and active (anodic) areas, very different electrically, may co-exist very close to one another. Further experimental work is necessary to separate various effects, such as ohmic drops, salt film formation and changes in chemical composition of the solution inside the cells[25,26].

Further clarification is also necessary of the stage of local breakdown of the passive film by aggressive ionic species, such as chlorides. To achieve this, a knowledge of the nature and behaviour of passive films is necessary[27]. Recently developed surface analysis techniques[28] seem to be the most appropriate for this type of investigation. To date, the points which have been clarified are: the beneficial effect of chromium enrichment in

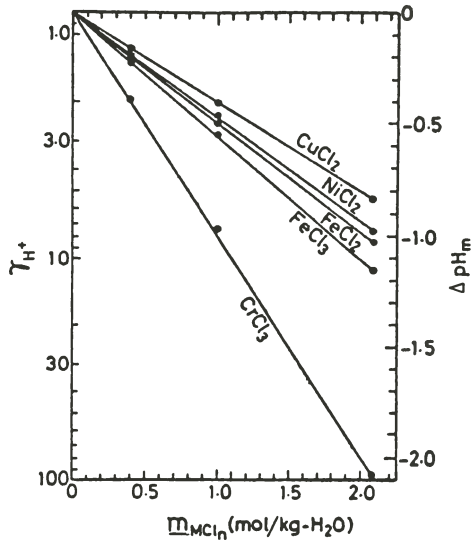

FIG. 12 - Activity coefficient of hydrogen ion, γ_{H^+}, in HCl (0.1 m) + MCl_n (m) solution[24].

passive films of stainless steels, the important role played by water in determining the protective and repairing properties of the film[27,29]. The last mentioned property is related to the availability of "free" water molecules in solution[2]. Without any doubt, important for the design of new alloys is an understanding of the effects of various alloying elements on the resistance of the film to breakdown, on the anchorage to the base alloy and on the re-passivation properties. Finally, the specific mechanism of action of many anionic species (whether aggressive or not) on the "breakdown" or "protection" of passive films needs clarification[30-32].

Received January 23rd, 1980

REFERENCES

1) B.F. BROWN: Corrosion, 26, 249 (1970).
2) G. FAITA, F. MAZZA, G. BIANCHI: "Localised Corrosion", Williamsburg (USA), 1971, NACE 3, p. 34.
3) H.W. PICKERING, R.P. FRANKENTHAL: J. Electrochem. Soc., 119, 1297 (1972).
4) R.P. FRANKENTHAL, H.W. PICKERING: J. Electrochem. Soc., 119,

1304 (1972).
5) J. NEWMAN: "Localised Corrosion", Williamsburg (USA), 1971, NACE 3, p. 45.
6) J. NEWMAN: "Electrochemical Systems", Prentice-Hall, Englewood-Cliffs, 1973.
7) F.P. FORABOSCHI: "Fenomeni di trasporto", Scuola di Elettrochimica Industriale, S. Felice del Benaco(BS), Italia, 10-21 Settembre 1979.
8) B.G. ATEYA, H.W. PICKERING: "Hydrogen in Metals", I.M. Bernstein, A.W. Thompson, Eds., (USA), 1974, p. 207.
9) J.R. GALVELE: J. Electrochem. Soc., 123, 464 (1976).
10) K.J. VETTER: "Electrochemical Kinetics", Academic Press, New York, 1961, p. 180.
11) B. VICENTINI, D. SINIGAGLIA, G. TACCANI: Werkst.Korros., 22, 916 (1971).
12) B. VICENTINI: Werkst. Korros., 25, 593 (1974); B. VICENTINI, D. SINIGAGLIA, G. TACCANI: Corros. Sci., 15, 479 (1975).
13) J. NEWMAN, D.N. HANSON, J. VETTER: Electrochim. Acta, 22, 829 (1977).
14) J.L. CROLET, J.M. DEFRANOUX: Corrosion Sci., 13, 575 (1973).
15) J.L. CROLET, L. SERAPHIN, R. TRICOT: Rev. Métall. (Paris), 12, 927 (1975).
16) J.W. OLDFIELD, W.H. SUTTON: Br. Corros. J., 13, 13 (1978).
17) J. MANKOWSKI, Z. ZSKLARSKA SMIALOWSKA: Corros. Sci., 15, 493 (1975).
18) J.W. OLDFIELD, W.H. SUTTON: Br. Corros. J., 13, 104 (1978).
19) J.W. OLDFIELD, W.H. SUTTON: Submitted for publication to Br. Corros. J.
20) T. SUZUKI, M. YAMABE, Y. KITAMURA: Corrosion, 29, 18 (1973).
21) M.H. PETERSON, T.J. LENNOX, R.F. GROOVER: Mater. Prot., 19, 23 (1970).
22) G. KARLBERG, G. WRANGLEN: Corros. Sci., 11, 499 (1971).
23) M. MAREK, R.F. HOCHMAN: Corrosion, 30, 208 (1974).
24) Y. HISAMATSU: Joint Japan-USA Seminar on Passivity and its Breakdown on Iron and Iron Base Alloys, NACE, Houston (USA) 1976, p. 99.
25) K.J. VETTER, H.H. STREHBLOW: "Localised Corrosion", Williamsburg (USA), 1971, NACE 3, p. 240.
26) I. MATSUSHIMA, J. SAKAI, K. MASAMURA; Proceedings 7th International Congress on Metallic Corrosion, Rio de Janeiro, Brasil, 1978, p. 506.
27) G. OKAMOTO: Corros. Sci., 13, 471 (1973).
28) D.T. LARSON: Corros. Sci., 19, 657 (1979).
29) H. SAITO, T. SHIBATA, G. OKAMOTO: Corros. Sci., 19, 693 (1979).
30) U.R. EVANS: Electrochim. Acta, 16, 1825 (1971).
31) A.J. ROSTRON: Corros. Sci., 19, 123 (1979); ibid, 19, 321 (1979).
32) J. KRUGER: Joint Japan-USA Seminar on Passivity and its Breakdown on Iron and Iron Base Alloys, NACE, Houston(USA),1976,p.91.